



Republic of Iraq

Ministry of Higher Education and Research

University of Babylon Faculty of

Materials Engineering

**Study the Properties of Alumina After
Adding Different Ratio of Titania and
Megnesia**

Graduation project submitted to materials Engineering_
University of Babylon

By:

Mohammed Ali Shaheed

Supervisor By

**Dr. prof.
Elham Abdul mageed**

**Dr.
Aseel Hadi**

2022-2023

بِسْمِ اللَّهِ الرَّحْمَنِ الرَّحِيمِ
﴿وَلَمَّا بَلَغَ أَشُدَّهُ وَاسْتَوَىٰ آتَيْنَاهُ حُكْمًا وَعِلْمًا
وَكَذَٰلِكَ نَجْزِي الْمُحْسِنِينَ﴾ (١٤)

صدق الله العظيم

سورة القصص (الآية ١٤)

Supervisors Certification

We certify that this thesis, entitled (*Study The Properties of Alumina After Adding Different Ratio of Titania and Megnesia*) was prepared by the student (**Mohammed Ali Shaheed**), Under our supervision, in partial fulfillment of the requirements for a bachelor's degree in Ceramics and Building Materials Engineering/ College of Materials Engineering.

Signature

Supervisor

Prof. Dr. Elham Abd Al-Majeed

Date 7 / 6 / 2023

Signature

Prof.Dr. Mohsin Abbas Aswad
Head of ceramic and building material department

Date 7 / 6 / 2023

الاهداء

الى من بلغ الرسالة وأدى الأمانة... ونصح الأمة... الى نبي الرحمة
ونور العالمين.. محمد (صل الله عليه وآله وسلم)
الى من كلفه الله بالهبة والوقار... الى من علمني العطاء بدون
انتظار.. الى من حمل اسمه بكل افتخار.. والدي العزيز
الى ملاكي في الحياة.. الى معنى الحب والى معنى الحنان والثقاني... الى
بسمته الحياة وسر الوجود... الى من كان دعائها سر لجاحي وحنانها
بلسر جراحني... الى أغلى الحبايب والديتي العزيزة.
الى من وقف الى جانبي وساندني دوماً.
الى كل من علمني حرفاً أصبح ينير الطريق امامي...
الى كل من ضحى بدمه من اجل الوطن... الى قواتنا في الحشد الشعبي
والجيش العراقي..

الشكر والتقدير

لابد لنا ونحن نخطو خطواتنا الأخيرة في الحياة الدراسية من وقفه نعود بها الى اعوام قضيناها في رحاب جامعة بابل \ كليه هندسة المواد \ قسم هندسة السيراميك ومواد البناء مع أستاذتنا الكرام الذين قدموا لنا الكثير باذلين بذالك جهوداً كبيرة في بناء جيل الغد لتعش الامة من جديد . شكر مقدم الى مختبرات كلية هندسه المواد \ قسم السيراميك لتسهيلهم متطلبات المشروع . وقبل ان نمضي نقدم أسمى آيات الشكر والامتنان والتقدير والمحبة الى الذين حملوا اقدس رسالة في الحياة .

الى جميع اساتذتنا الافاضل .

واخص بالتقدير والشكر استاذي المشرف :

الاستاذ المساعد الدكتور الهام عبد المجيد

والدكتور اسيل هادي

List of Contents

Subjects	Page No.
Abstract English	
Abstract Arabic	
Chapter one: Introduction	1-4
1.1. Introduction	1-3
1.2. Objective of the current study	3
1.3. The aim	4
Chapter Two: Theoretical part	5-22
2.1. Introduction	5
2.2. Powder Metallurgy	5-6
2.3. Oxides	6-9
2.4. Literature reviews	9-10
2.5. Properties of (AL ₂ O ₃ , Tio ₂ , MgO)	10-13
2.6. Compacting	13-15
2.7. Sintering	15-16
2.8. Sintering mechanisms	16-19
2.9. Sintering stages	19- 21
2.10. Densification rate curves	21-22
Chapter Three: Experimental part	32-32
3.1. Introduction.	23
3.2. Used materials	23
3.3. Preparing samples	23-26
3.4. Tests	27-32
Chapter Four: Result and Discussion	33-43
4.1. Introduction	33
4.2. X-Ray Test	33-34
4.3. Particle size for powders	35-36
4.4. Physical Tests	36-40
4.5. Mechanical Tests	40-43
Chapter five: Conclusion and Recommendation	43
5.1. Conclusion	43
5.2. Recommendations and suggestions for future work	43

References	44-47
-------------------	--------------

List of Tables

Title	Page No.
Table (2-1) properties of Alumina	11
Table (2-2) properties of Titanium Dioxide	12
Table (2-3) properties of magnesium oxide	13
Table (3-1) the Ratio of the component	23
Table (4-1) Results of density	36
Table (4-2) Results of porosity	37
Table (4-3) Results of shrinkage	38
Table (4-4) Results of absorption	39
Table (4-5) Results in Vickers hardness	40
Table (4-6) The relation between the samples (AL ₂ O ₃) and wear	41
Table (4-7) The relation between the samples (AL ₂ O ₃ + Tio ₂ + MgO) and wear	42
Table (4-8) The relation between the samples (AL ₂ O ₃ + Tio ₂) and wear	42

List of figure

Title	Page No.
Figure (2-1) structure of alpha- alumina	7
Figure (2-2) show titanium dioxide polymorphs	8
Figure (2-3) stages of compaction, tap density, rearrangement and green density.	14
Figure (2-4) schematic of two possible paths by which a collection of particles can lower its energy.	17
Figure (2-5) row of initially spherical particle	18
Figure (2-6) neck of formation	19
Figure (2-7) coarsening resulting from low coordination number.	20

Figure (2-8) typical densification curve.	22
Figure (3-1) powder of AL ₂ O ₃ + Tio ₂ + MgO	24
Figure (3-2) Electrical mixer	24
Figure (3-3) pressuring method	25
Figure (3-4) drying oven	26
Figure (3-5) samples after sintering	26
Figure (3-6) A- shimadzu 6000 X-Ray, B- working	28
Figure (3-7) batter size 2000 laser particle size analyzer	29
Figure (3-8) microhardness device	32
Figure (4-1) X-Ray for AL ₂ O ₃	33
Figure (4-2) X-Ray for Tio ₂	34
Figure (4-3) X-Ray for MgO	34
Figure (4-4) particle size for AL ₂ O ₃	35
Figure (4-5) Particle size for Tio ₂	35
Figure (4-6) Particle size for MgO	36
Figure (4-7) the relation between the samples and density	37
Figure (4-8) the relation between the samples and porosity	38
Figure (4-9) the relation between the samples and shrinkage	39
Figure (4-10) the relation between the samples and absorption	40
Figure (4-11) the relation between the samples and hardness	41
Figure (4-12) the relation between the samples (AL ₂ O ₃) and wear	41
Figure (4-13) the relation between the samples (AL ₂ O ₃ + Tio ₂ + MgO) and wear	42
Figure (4-14) the relation between the samples (AL ₂ O ₃ + Tio ₂) and wear	42

Abstract

Powder technology (P/T) process includes compacting of fine powders followed by sintering process to get products of desired properties.

Several factors affected sintering; however, the most significant are time and temperature, with temperature being the most important single variable.

In this research study the effect of adding Ti_2O and MgO on properties of Al_2O_3 system . Some physical and mechanical properties have been studied, such as density, porosity, shrinkage and absorption, hardness and wear.

Three samples were prepared such as A,B, and C, where A indicated to Pure alumina powder as sample (A) with (100%) alumina,(B) sample indicated to alumina of (80%) mixing with weight percent of (20 %) titania. Finally (C) sample indicated to mixing of (60 %) alumina, (20 %) titania and (20 %) magnesia .

XRD tests and particle size were carried out for the three different powders.

Pure alumina, mixture of alumina and titania, mixture of alumina, titania and magnesia were prepared by mixing and compacting by cold pressing at a pressure of (10) MPa, and sintering at temperature about (1200 °C), a good results have been got for the mechanical, physical properties.

To evaluate the performance of the prepared material, several tests were conducted such as physical testes which include porosity, density , shrinkage and absorption of these samples also mechanical test such as hardness and wear were carried out.

Physical properties play good role in this study, density, were about (2.4 g/cm³), (2.96 g/cm³), and (2.98 g/cm³) respectively for samples (A), (B), and (C), and , porosity were about (1.1%), (0.88 %) and (0.87%) respectively for three samples. Shrinkage for sample(A) is (-2.96%) and (-2.6%) (-1.91%) respectively for samples (B) and (C) . finally absorption for three samples were (45%), (43%) and (42%).

The increase in hardness of sample (C) compared to other samples with value of (19.81) for sample (C). Wear also play a good roll in this study , the value of three samples decrease as hardness increase.

الخلاصة

تتضمن عملية الباودر تكنولوجي (P / T) كبس المساحيق الدقيقة تليها عملية تلييد للحصول على المنتجات المرغوبة .

هناك عدة عوامل تؤثر على التلييد. ومع ذلك ، فإن الأكثر أهمية هي الوقت ودرجة الحرارة ، ودرجة الحرارة هي من العوامل المهمة.

في هذا البحث تم دراسة تأثير إضافة Ti_2O و MgO على خصائص نظام Al_2O_3 . ودراسة بعض الخواص الفيزيائية مثل المسامية والكثافة والانكماش والامتصاص، و الميكانيكية مثل الصلادة والبلى.

تم تحضير ثلاث عينات مثل (أ) ، (ب) و (ج) حيث أشارت العينة (أ) إلى مسحوق الألومينا النقي بنسبة (100%) ألومينا ، عينة (ب) المشار إليها للألومينا بنسبة (80%) مخلوطة بوزن نسبة (20%) تيتانيا. أخيراً أشارت العينة (ج) إلى خلط (60%) من الألومينا بنسبة (20%) تيتانيا و (20%) مغنيسيا.

تم إجراء اختبارات للمسحوق مثل XRD وحجم الحبيبات للمساحيق الثلاثة المختلفة.

تم تحضير عينات من الألومينا النقية ، خليط من الألومينا والتيتانيا ، خليط من الألومينا ، التيتانيا والمغنيسيا عن طريق الخلط والكبس على البارد حيث ان الكبس كان عند حمل (10) ميغا باسكال ، والتلييد عند درجة حرارة حوالي (1200 درجة مئوية) ، تم الحصول على نتائج جيدة للخواص الفيزيائية و الميكانيكية.

لتقييم أداء المواد المعدة ، تم إجراء عدة اختبارات مثل الخصائص الفيزيائية والتي تشمل الكثافة ، المسامية ، الانكماش والامتصاص. فضلاً عن ذلك تلعب الخصائص الميكانيكية دوراً جيداً في هذه الدراسة مثل الصلادة والبلى.

كانت قيم الكثافة g/cm^3 [(2.4) و (2.96) و (2.98)] على التوالي للعينات (أ) و (ب) و

(ج)

وكانت المسامية حوالي (1.1%) و (0.88%) و (0.8%) على التوالي لثلاثة عينات. الانكماش للعينة (أ) هو (-2.96%) و (-2.46%) (-1.91%) على التوالي للعينات (ب) و (ج) ، وأخيرا الامتصاص كانت القيم للعينات الثلاث على التوالي (45%) و (43%) و (42%).

اما الخواص الميكانيكية نجد زيادة صلادة العينة (ج) مقارنة بالعينات الأخرى بقيمة (19.81) للعينة (ج). البلى لعب دور مهم في هذه الدراسة , نجد ان قيم البلى للعينات الثلاثة تقل مع زيادة الصلادة.

Chapter one

Introduction

Introduction

1.1 Introduction

The word 'ceramic', is derived from the Greek speech for pottery, describes a wide range of materials that include glass, porcelain, brick, pottery, cement and concrete. The use of ceramics - as fired clay - goes back to about 6000BC [1]. Ceramic materials can be defined as inorganic materials constituted by the combination of metallic and nonmetallic elements whose properties depend on the way in which these elements are linked [2].

Ceramic materials can be divided into two large groups: traditional ceramics and technical or advanced ceramics. Traditional ceramics can be defined as those that are based on silicates, among which are cement, clay products, and refractories. Traditional ceramic materials are made with raw materials from natural deposits such as clay materials [3]. The second group, technical or advanced ceramics, Advanced ceramics are materials tailored to possess exceptional properties (superior mechanical, corrosion/oxidation resistance, thermal, electrical and magnetic properties) by controlling their composition and internal structure [4, 5]. They are subdivided into structural ceramics, electrical ceramics, ceramic coatings, chemical processing and environmental ceramics (filters and membranes) [6]. Advanced ceramics, also referred to as engineering ceramics [5].

Ceramic materials consist of at least two elements, which make their crystal structures more complex than those of simple metals [7]. Ceramics are usually characterized by high melting temperature, low coefficients of thermal expansion, low electrical conductivity and are strong in compression, but brittle [2]. There is basically no dislocation motion in ceramics, which makes their mechanical behavior primarily different from that of metals; mechanical properties of ceramics are determined by crack initiation and propagation [8]. Ceramics find wide applications as insulators (electrical and thermal), structure materials (bricks and tiles) .

Oxide is large and important class of chemical compounds in which oxygen is combined with another element. With the exception of

the lighter inert gases (helium [He], neon [Ne], argon [Ar], and krypton [Kr]), oxygen (O) forms at least one binary oxide with each of the elements.

Both metals and nonmetals can attain their highest oxidation states (i.e., donate their maximum number of available valence electrons) in compounds with oxygen. The alkali metals and the alkaline earth metals, as well as the transition metals and the post transition metals (in their lower oxidation states), form ionic oxides—i.e., compounds that contain the O^{2-} anion. Metals with high oxidation states form oxides whose bonds have a more covalent nature. Nonmetals also form covalent oxides. A smooth variation from ionic to covalent in the type of bonding in oxides is observed as the periodic table is traversed from the metals on the left to the nonmetals on the right. This same variation is observed in the reaction of oxides with water and the resulting acid-base character of the products. Ionic metal oxides react with water to give hydroxides (compounds containing the $-OH$ ion) and resultant basic solutions, whereas most nonmetal oxides react with water to form acids and resultant acidic solutions [5].

Aluminium oxide is a chemical compound of aluminium and oxygen with the chemical formula Al_2O_3 . It is the most commonly occurring of several aluminium oxides, and specifically identified as aluminium(III) oxide. It is commonly called alumina and may also be called aloxide, aloxite, or alundum depending on particular forms or applications. It occurs naturally in its crystalline polymorphic phase $\alpha-Al_2O_3$ as the mineral corundum, varieties of which form the precious gemstones ruby and sapphire. Al_2O_3 is significant in its use to produce aluminium metal, as an abrasive owing to its hardness, and as a refractory material owing to its high melting point.

It is a naturally occurring common compound. It is useful in a variety of industries, most importantly in the manufacture of aluminium. The substance is used in the manufacture of industrial ceramics. Corundum, its most common crystal form, also has several variants of gem-quality.

Magnesium oxide (MgO) and hydroxide [$Mg(OH)_2$] are conventionally considered insoluble in water and stable at high temperatures. However, in this study, we found significant dissociation of

MgO and Mg(OH)₂ into ions when they were immersed in different physiologically relevant solutions in the form of 20-nm and 10-nm nanoparticles respectively, under standard cell culture conditions in vitro, i.e., a 37 °C, 5% CO₂/95% air, sterile, humidified environment. The change in Mg²⁺ ion concentrations and pH measured in the physiologically relevant solutions (e.g., Dulbecco's modified Eagle's Medium (DMEM), simulated body fluid (SBF), relevant chloride solutions, and deionized water) confirmed their dissociation. Possible mechanisms and contributing factors for dissociation of MgO and Mg(OH)₂ nanoparticles were discussed. The evidence suggests that nucleophilic substitution of OH⁻ by Cl⁻ in Mg(OH)₂ is energetically unfavorable and it is more likely that Cl⁻ plays a role in the stabilization of intermediate forms of MgO and Mg(OH)₂ as it dissociates. The pH and buffering capability of the immersion solutions might have played the most significant role in dissociation of these nanoparticles when compared with the roles of chloride (Cl⁻), proteins, and different buffering agents. This article provided the first evidence on the dissociation of MgO and Mg(OH)₂ nanoparticles in physiologically relevant conditions and elucidated possible factors contributing to the observed behaviors of these nanoparticles in vitro, which is important for their potential medical applications in vivo.

1.2. Objectives of the current study

Alumina (Al₂O₃), titania (TiO₂) and magnesia (MgO) are of great importance for applications in various machinery and transportation system, especially in thermal applications, aerospace, automobile products and several applications due to their superior physical and chemical performances.

In view of facts mentioned above, the objectives of the current work are:

- (1) Alumina was used as a basic material in this research, then proportions of titania and magnesia were added to know the effect of these materials on different properties.
- (2) Study the effect of these additives on the several properties such as hardness, wear, porosity, density, shrinkage and absorption.

1.3. The aim

Aim and the main purpose of this research is to study the properties of the samples that were prepared in laboratories, ceramic as alumina was used as a basic material in this research, then amounts of titania and magnesia were added to know the effect of these materials on different properties to investigate some properties of composite materials to find out the field in which we can use these materials by examining some of their properties.

Then notice the development in mechanical, and physical properties.

The present research is an attempt to understand the influence of addition (% of titania) and (% of magnesia) to matrix of alumina.

Chapter two

Theoretical part

Theoretical part

2.1 Introduction

This chapter focuses on titanium oxide, alumina, magnesium oxide, their properties and applications and powder metallurgy.... etc.

2.2 Powder Metallurgy

The powder metallurgy process consists of mixing powder, compacting the mixture in a die and then sintering or heating the resultant shape in a controlled atmosphere. Powder metallurgy is a highly developed method of manufacturing ferrous and nonferrous materials. This process is cost effective in producing simple or complex part in manufacturing rates which can range from a few hundred to several thousand parts per hour. Due to high cost of die and equipment this process is suitable for mass production only [25]. The basic steps involved in the production process are given below:

- Mixing and blending – Powder are mixed thoroughly and blended to ensure desired property.
- Preparation of powder or powders of desired composition.
- Compacting the powders into desired shape and size and providing strength to the parts.
- Sintering – Green compacts are heated at elevated temperature to impart strength [25].

2.2.1 Advantages and disadvantages of power metallurgy

The Power Metallurgy Advantages are:

1. Elimination or reduction of machining.
2. High production rates.
3. Complex shapes.
4. Wide variations in compositions.
5. Wide property variations.
6. Scrap is eliminated or reduced.
7. High tolerance parts possible with minimum processing [26].

The disadvantages of power metallurgy:

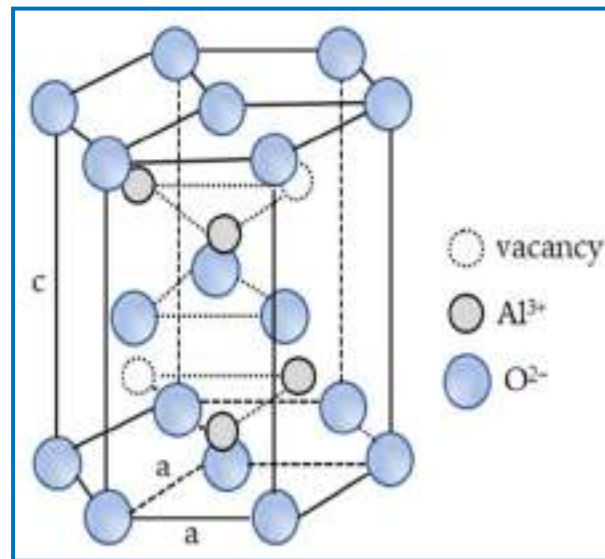
- 1- Dimensional changes during sintering
- 2- High material cost
- 3- Size and shape limitations
- 4- High tooling costs
- 5- Density variations
- 6- Porosity.
- 7- Health and safety hazards [26].

2.3. Oxides

2.3.1 Alumina (Al_2O_3)

The alumina exists with different phases depending on the alumina purity and its mechanical and physical properties. The most important, and common, alumina polymorphs (crystalline phase) are denoted as (α , γ , θ , and κ) [5]. The α phase is thermodynamically stable polymorph (as shown in figure (2-2)) and occurs naturally as corundum or sapphire, while the other phases are metastable in bulk form (but can still be produced in certain processes where thermal equilibrium is not reached, e.g., thin film growth). The differences in properties between the phases make them important in different applications. For example, the α and κ phases are widely used as wear resistant coatings due to their high hardness and thermal stability, while γ and θ -alumina are more suited for catalytic applications due to their lower surface energies, leading to larger active surface areas available for catalytic reactions. Crystalline phase are responsible for different properties of alumina yet dopants also effects on alumina phase stability. As an atom of the alumina lattice is substituted by another element, the energy of the lattice would change due to differences in chemical bonding and/or size of the substituting atom compared to the original. It has been shown that it is possible to increase or decrease the relative stability of the α -alumina and even make it less stable than the θ alumina by dopant atoms [18]. Consequently, the results predicted that it should be possible to control the thermal stability of doped alumina thin films in order to increase the thermal stability of metastable alumina phases. However, it is difficult, to predict the exact effect of doping in an experimental situation, since it was also shown that phase separations of the doped alumina are energetically favored, and

will most likely occur at elevated temperatures. The common alumina polymorphs formed within typical synthesis temperatures range from room temperature up to about 1000°C. This complicates the study and growth of alumina, since it becomes difficult to control the process so that the desired phase is achieved. All alumina phases are involved in transformation sequences, which all have in common that they end in α phase alumina at high temperature. Transformations into α phase are irreversible and typically take place at above 1000°C [18].



Figure(2-1). Structure of alpha-alumina (α -Al₂O₃). [19].

Alumina shares several characteristics with other polycrystalline ceramic materials, such as moderate tensile and bending resistance and the brittle fracture behavior, which is the main disadvantage of the mechanical properties of alumina[20].

The strong chemical bonds in alumina are the roots of several characteristics such as the low electric and thermal conductivity[8], the high melting point that makes it practically impossible to shape alumina by casting, and the high hardness that characterizes this material and makes its machining complex and costly.

2.3.2 Titanium Dioxide (TiO₂)

Titanium dioxide, alternatively, referred to as titania, is a found in nature titanium oxide. It is a versatile material that can be used for a variety of purposes [10]. (TiO₂) is being used as a photocatalyst relatively

low cost, non-toxicity, and chemical inertness[11]. TiO_2 is used in many industry sectors, such as airplane, sporting events, paint (to impart a glossy finish and rich intensity of color and as a replacement for metal lead), cosmetics (UV) safety in sunscreens and a group of industries [12,13]. Due to its sterilizing and anti-fouling properties, (TiO_2) is utilized to cover glazing. Through a vigorous catalytic reaction, the (TiO_2) will degrade and destroy organic dirt. Additionally, it is hydrophilic, allowing water to flow uniformly across its surfaces [14]. TiO_2 is a white color found in all kinds of paints, printing ink, plastics, paper, synthetic fibers, rubber, condensers, painting colors and crayons, ceramics, electronic components and cosmetics [15]. The great efforts devoted to the research on TiO_2 material produced many promising uses in areas which range from photovoltaics and photocatalysis to photo-electrochromic and sensors [15]. These uses can be generally classified into "energy" and "environmental" types, many of types rely not only on the properties of the TiO_2 material itself but also on the changes in the TiO_2 material host (e.g., with inorganic and organic dyes) . Titanium dioxide utilizes intense for lowering air pollution when applied to outdoor surfaces [16]. The titanium dioxide polymorphs are rutile, anatase and brookite [17].

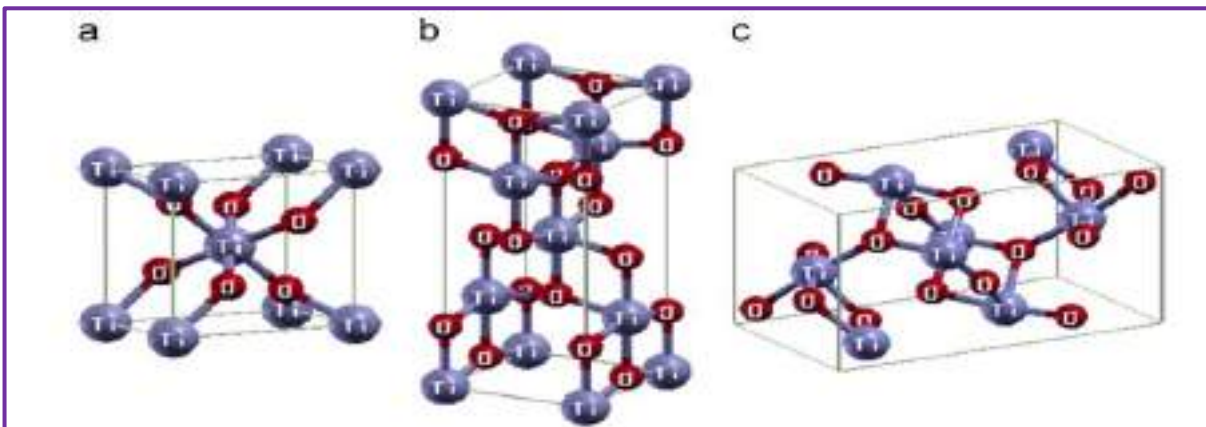


Figure (2.2) shows titanium dioxide polymorphs(a) Rutile ,(b) Anatase (c) Brookite [17].

2.3.3 Magnesium Oxide (MgO)

Magnesium oxide is an ionic ceramic which is mainly used for its refractory properties, as an exceptionally important inorganic material,

has found wide application in many fields including catalysts, adsorption and separation, chemical sensing, electrical and optical devices, superconductor products [22], furnaces and flame retardants as well as a compound for some technical ceramics for the construction industry (e.g., cements) [23]. due to its unique surface basic property as well as nontoxic and environmentally friendly nature. Over the past decades, many protocols such as the sol–gel route, the precipitation method, the hydrothermal method, chemical vapour deposition, precursor decomposition, and soon have been developed to fabricate meso-, micro- and nano-structured MgO. In recent years, numerous studies have demonstrated that the change in the morphology of MgO can alter its surface properties, which was formerly considered constant. For example, the catalytic performance of MgO was closely related with its shape, illustrating an apparent morphology-dependent phenomenon [22].

2.4 Literature Reviews

Ritwik and Goutam ,2000 studied three different spinel compositions with MgO:Al₂O₃ molar ratios 2:1, 1:1 and 1:2 using TiO₂ as an additive up to 2 wt.%. Solid state reaction sintering technique was employed for all the compositions in the temperature range of 1550–1650°C. Attrition milling was done for the reduction of particle size. Sintered products were characterized in terms of densification and shrinkage studies, phase analysis, strength evaluation both at ambient temperature and at elevated temperature. The results showed that TiO₂ improved the density of alumina rich and stoichiometric spinels sintered at 1550°C. TiO₂ up to 2 wt.% had no influence on the phase constituents of different spinels, Addition of TiO₂ showed only some marginal changes in cold strength values [27].

Liang Li ,2021 showed that MgO-Al₂O₃-SiO₂ composite ceramics are widely used in high-temperature filter materials, refractories, catalyst carrier materials and insulating materials because of their low coefficient of thermal expansion, good high-temperature stability and ceramics, it is more important to select a suitable mineralizer in order to effectively reduce the sintering temperature of MgO-Al₂O₃-SiO₂ composite ceramics and improve the properties of MgO-Al₂O₃-SiO₂ composite ceramics. In this experiment, fused magnesia, Al₂O₃ powder and

ferrosilicon ash powder were used as main raw materials. Meanwhile, Cr_2O_3 powder, ZrO_2 powder and TiO_2 powder were selected as mineralizers. $\text{MgO-Al}_2\text{O}_3\text{-SiO}_2$ composite ceramics were prepared by the semi-dry pressing method. The effects of different mineralizers on the sintering properties of $\text{MgO-Al}_2\text{O}_3\text{-SiO}_2$ composite ceramics were studied. The experimental results show that the addition of TiO_2 powder can promote the sintering of $\text{MgO-Al}_2\text{O}_3\text{-SiO}_2$ composite ceramics. Moreover, the sintering performance of $\text{MgO-Al}_2\text{O}_3\text{-SiO}_2$ composite ceramics is better than that of $\text{MgO-Al}_2\text{O}_3\text{-SiO}_2$ powder. When the addition of ZrO_2 powder is 4%, it can promote the formation of periclase phase, refine grains and play a toughening effect, and the bending strength of $\text{MgO-Al}_2\text{O}_3\text{-SiO}_2$ composite ceramics reaches the maximum value of 19.3 MPa [28].

Oksana M. Borysenko *etal*, 2021 explained the information on the structure of the triple component system, in particular $\text{MgO-Al}_2\text{O}_3\text{-TiO}_2$ that serves as a basis for the production of thermal resistance materials. It was established that the triangulation of the $\text{MgO-Al}_2\text{O}_3\text{-TiO}_2$ system was changed in the three temperature intervals: in the temperature range lower than 1537 K TiO_2 existed as the polymorphous modification, i.e. anatase; in the temperature range from 1537K to 2076 K TiO_2 existed as a polymorphous modification in form of rutile and tialite was stable; and at the temperatures above 2076 K the availability of stoichiometric compound of Al_4TiO_8 was possible. In the temperature range lower than 1537 K the two-phase equilibria of $\text{Al}_2\text{O}_3\text{-MgTi}_2\text{O}_5$, $\text{MgTi}_2\text{O}_5\text{-MgAl}_2\text{O}_4$, $\text{MgTiO}_3\text{-MgAl}_2\text{O}_4$, and $\text{Mg}_2\text{TiO}_4\text{-MgAl}_2\text{O}_4$ were stable [29].

2.5. properties of (Al_2O_3 , TiO_2 , MgO)

2.5.1 Properties of Aluminium Oxide (Al_2O_3)

Typical alumina characteristics include:

- Good hardness and wear resistance.
- Good strength and stiffness.
- Good corrosion resistance.
- Good thermal stability.
- Excellent dielectric properties (from DC to GHz frequencies)

- Low dielectric constant.
- Low loss tangent.

Table (2-1) properties of alumina.

96% Aluminum Oxide			
Mechanical	Units of Measure	SI/Metric	(Imperial)
Density	gm/cc (lb/ft ³)	3.72	(232.2)
Porosity	% (%)	0	(0)
Color	—	white	—
Flexural Strength	MPa (lb/in ² x10 ³)	345	(50)
Elastic Modulus	GPa (lb/in ² x10 ⁶)	300	(43.5)
Shear Modulus	GPa (lb/in ² x10 ⁶)	124	(18)
Bulk Modulus	GPa (lb/in ² x10 ⁶)	172	(25)
Poisson's Ratio	—	0.21	(0.21)
Compressive Strength	MPa (lb/in ² x10 ³)	2100	(304.5)
Hardness	Kg/mm ²	1100	—
Fracture Toughness K _{1c}	MPa•m ^{1/2}	3.5	—
Maximum Use Temperature (no load)	°C (°F)	1700	(3090)
Thermal			
Thermal Conductivity	W/m•°K (BTU•in/ft ² •hr•°F)	25	(174)
Coefficient of Thermal Expansion	10 ⁻⁶ /°C (10 ⁻⁶ /°F)	8.2	(4.6)
Specific Heat	J/Kg•°K (Btu/lb•°F)	880	(0.21)
Electrical			
Dielectric Strength	ac-kv/mm (volts/mil)	14.6	(365)
Dielectric Constant	@ 1 MHz	9.0	(9.0)
Dissipation Factor	@ 1 kHz	0.0011	(0.0011)
Loss Tangent	@ 1 kHz	—	—
Volume Resistivity	ohm•cm	>10 ¹⁴	—

2.5.2 Properties of (TiO₂)

Titanium dioxide, also known as titanium(IV) oxide or titania /tar'teɪniə/, is the inorganic compound with the chemical formula TiO. When used as a pigment, it is called titanium white. It is a white solid that is insoluble in water, although mineral forms can appear black. As a pigment, it has a wide range of applications, including paint, sunscreen, and food coloring.

Synthetic TiO_2 is mainly produced from the mineral ilmenite. Rutile, and anatase, naturally occurring TiO_2 , occur widely also, e.g. rutile as a 'heavy mineral' in beach sand. Leucoxene, fine-grained anatase formed by natural alteration of ilmenite.

Table (2-2) properties of Titanium Dioxide

TiO_2	Titanium dioxide
Molecular Weight/ Molar Mass	233.38 g/mol
Density	4.5 g/cm ³
Boiling Point	1,600 °C
Melting Point	1,580 °C

2.5.3. Properties of (Mgo)

- Atomic Symbol: Mg
- Atomic Number: 12
- Element Category: Alkaline metal
- Density: 1.738 g/cm³ (20°C)
- Melting Point: 1202 °F (650 °C)
- Boiling Point: 1994 °F (1090 °C)
- Moh's Hardness: **2.5**

Table (2-3) properties of magnesium oxide.

Property	Minimum value (S.I.)	Maximum value (S.I.)	Units (S.I.)
Density	3.54	3.58	mg/m ³
Compressive Strength	833.3	1666.6	MPa
Ductility	0.00038	0.00041	
Fracture Toughness	2.7	2.8	MPa.m ^{1/2}
Hardness	5000	7000	MPa
Shear Modulus	92	122	GPa
Tensile Strength	83.3	166.7	MPa
Young's Modulus	270	330	GPa
Melting Point	3080	3135	K
Thermal Conductivity	30	60	W/m. K
Thermal Expansion	9	12	10 ⁻⁶ /K
Dielectric Constant	6.8	9.6	

2.6. Compacting

Powder compaction can be summed up as the operation that provides shape, dimensional control, desired density and strength for subsequent handling. Conventional compaction occurs in the following manner, as shown in figure 2-3. Initially, as pressure is applied, the loose arrays of particles are packed closer and particle bridging is eliminated. At this stage the density attained is at most equivalent to the tap density. As the pressure is further increased the contact area grows through rearrangement and sliding. At high pressures the contact area increases through plastic deformation. The inter-particle bonds develop through cold welding, weak attractive forces and mechanical interlocking. The strength developed at this stage is called the green strength, while the pressed density is termed the green density. Generally, due to interlocking, rounded but irregular large shaped particles result in the highest green strength. The higher the hardness of the particles the lower the green density. If the particles are small, the finer pores will require higher pressures to collapse and the pressed density will be low. In

general, characteristics that improve the green density is also improve the green strength .

All methods of compaction have the same goal, which is to achieve the desired shapes with minimal die wall-tool friction. This resulted in reduced tool wear and improved pressing efficiency. Compaction to be successful (i.e. uniform compact properties), the ratio of compact height (H) to the compact diameter (D) must not exceed five .

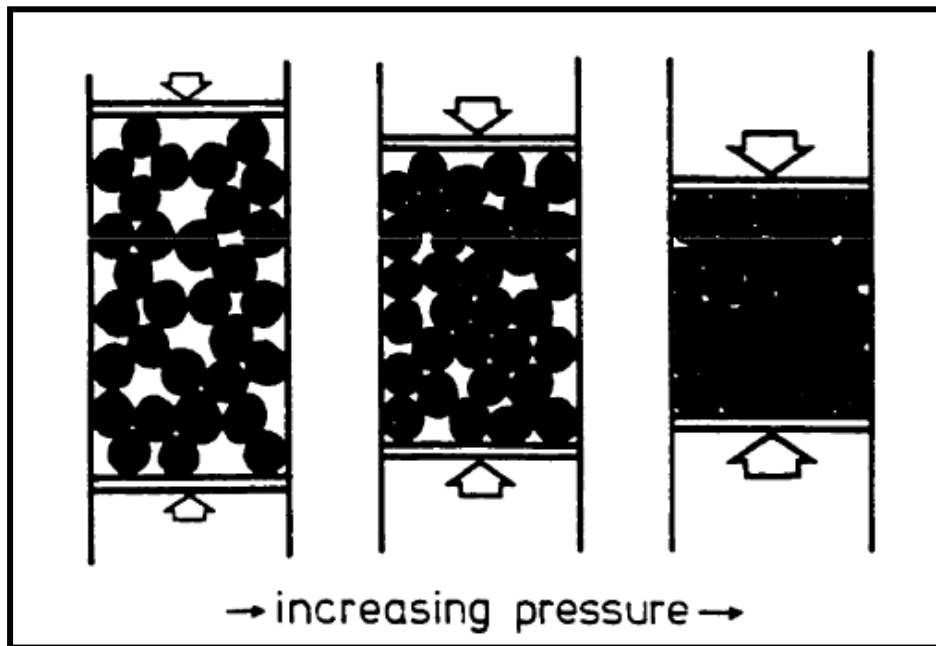


Figure 2-3 Stages of compaction, tap density, rearrangement and green density [2].

The green-state compact consists of powder particles pressed together. Although the green-state compacts look to the eye like any solid part, there are no bonds in the compact other than interparticle bonds created through the deformational forces that pressed the powder particles together. Consequently, the green-state compact is very fragile and susceptible to damage [7].

Ceramic powders are commonly pressed into dies to produce near-net shape "green" bodies prior to final sintering. Density gradients in the resulting compacts may cause distortion in the shape of the parts during sintering, necessitating expensive machining or grinding operations to obtain the desired final shape. Nonuniform shrinkage may even generate

internal stresses that are sufficiently large to cause fracture of the part during sintering. Equally importantly, these density gradients can result in green bodies that break during ejection from the die or that are too fragile to be handled [10].

2.7. Sintering

Sintering is a heating process in which a fine powder that has been formed into a shape is subsequently fired at temperature below melting point. The compact, when fired, densifies and becomes less or non-porous [10]. The powder particles form bonds at this temperature and the contact points between particles, which were originally formed under the mechanical pressure during compaction, increase in size and strength, improving mechanical properties [10].

The particle size has a great importance in P/T because it affects most of the properties. So the powders are divided into three distinct classes, sieve having the aperture of 44 micron, sub-sieve are smaller than the aperture of such a screen but greater than 1 micron and sub-micron or ultra-fine is smaller than 1 micron. Particle size is expressed by the diameter for spherical shaped particles and by the average diameter for non-spherical particles[].

Sintering is a thermal treatment that densification accompanies. Densification almost always requires shrinkage (in some cases zero changes or even growth). The shrinkage takes place as a result of materials being transported by one or more of several diffusion processes. This may involve a liquid or reactive liquid or diffusion at grain boundaries or through the volume of particles [11, 12].

Therefore, it is a densification process where porosity is usually reduced and the grain size increases significantly through mass transport. This is important because it allows an engineer to form a dense ceramic body at temperatures below the often very high melting temperature of the ceramic. For many properties such as strength, thermal conductivity and translucency, in order to reach a maximum value for a product. It is necessary to remove as much porosity as possible. A formed powder compact can be anywhere from 40% to 75% dense, with little strength. A sintered body can have much higher strengths and densities may exceeding 99% [10].

The ability to achieve dimensional tolerances in powder technology parts arises directly from the control of the sintering process and in particular shrinkage. Thus, a detailed understanding of the sintering process and the associated shrinkage is of considerable importance [2].

2.7. Sintering mechanisms

Sintering proceeds from various mass-transport mechanisms. These can be divided into surface transport and bulk transport mechanisms. In surface transport mechanisms, atoms move from the surface of one particle to the surface of another particle. In bulk transport mechanisms, atoms move from the particle interior to the surface. Surface transport mechanisms lead to neck growth without shrinkage or densification, while bulk transport mechanisms result in net particle movement, leading to shrinkage and densification. Densification means an increase in packing density. The surface transport mechanisms are surface diffusion and vapor transport. While, the bulk transport mechanisms are lattice diffusion, grain boundary diffusion, and viscous flow. In powders composed of different materials, chemical reactions (also called reactive process) may also provide additional mass-transport mechanisms [13].

Different mechanisms dominate at different points in the sintering process and different materials exhibit different mechanisms. For instance, viscous flow is the diffusion in the liquid phase and evaporation condensation (vapor diffusion) is in the gaseous phase. Evaporation condensation and surface diffusion are called non-densifying mechanisms because they do not contribute to the pore shrinkage. They only increase the cohesion of the grains by the increase in the grain contacts. On the other hand, mechanisms contribute to the decrease of the volume fraction of pores; i.e.; the shrinkage [14].

The compaction powder (called a green compact) has a large surface area relative to its volume. This surface area provides the driving force in sintering, which is the reduction of free surface energy resulting from the high surface area of the particles [14].

Solid state sintering may be performed by two alternative processes: namely one reduction of the total surface area by an increase in the average size of the particles, which leads to coarsening figure 2-3b, and

two reduction by elimination of solid / vapor interface and the creation of grain boundary area followed by grain growth, which leads to densification figure 2-4a [15].

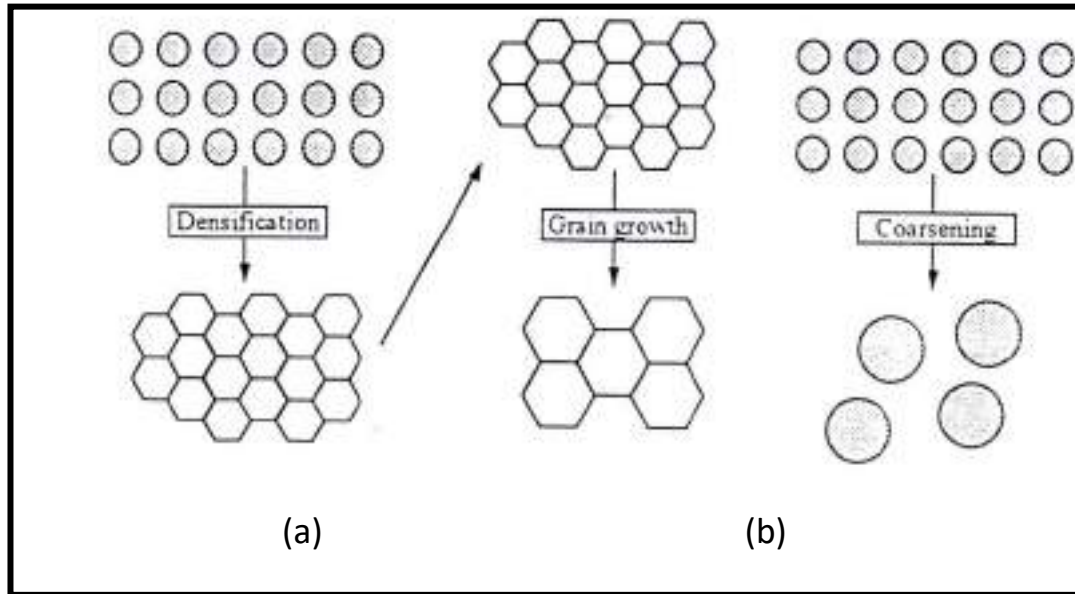


Figure 2-4 Schematic of two possible paths by which a collection of Particles can lower its energy [15].

These two mechanisms are usually in competition. If the ionic processes that lead to densification dominate, the pores get smaller and disappear with time and the compact shrinks. But if the atomic processes that lead to coarsening are faster, both the pores and grains coarsen and get larger with time [12,15].

Figure 2-5 shows neck growth with no shrinkage for simple array of spherical particles when the operating mechanism is a surface or vapor diffusion only. When a densifying mechanism is operating, both neck growth and densification take place as shown in the same figure [15].

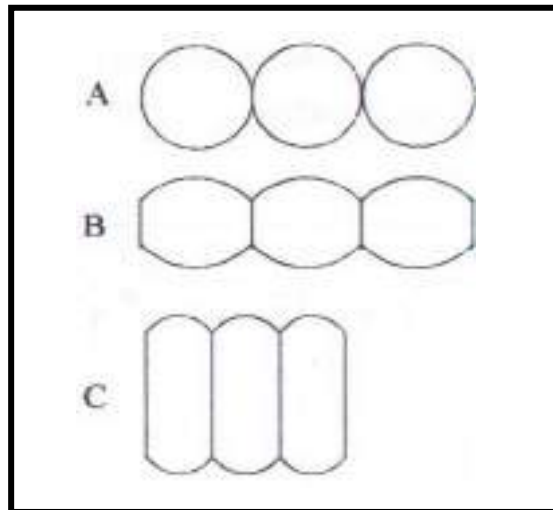


Figure 2-5 a. Row of initially spherical particle b. Neck growth and no shrinkage by surface or vapor phase diffusion, and c. The shrinkage when a densifying mechanism is operating [15].

A sintered part begins as a green compact, which is low-density, inhomogeneous and porous, and generally lacks in physical integrity. There is, however, a small degree of adhesion between adjacent particles [15].

During the final stages of sintering, in addition to the elimination of pores, a general coarsening of the microstructure by grain growth may occur. During coarsening, smaller particles disappear and larger particles grow. The average grain size often related to the primary particle size. An exception to this is if there is grain growth due to long sintering times or exaggerated or abnormal grain growth. Typically, ceramics with a small grain size are stronger than coarse-grained ceramics [15].

Sintering can occur either at atmospheric pressure or under isostatic or hydrostatic pressure. This pressure-assisted sintering increases the sintering rate, reduces sintering time, and reduces porosity in the final part. Generally It takes place at temperatures in excess of half the absolute melting temperature. If sintering takes place at temperatures high enough to higher than melting point of one of the component of the elementary powders, it is called liquid-phase sintering, sintering that takes place at lower temperatures without any melting of any component is called solid-state sintering [15].

2.8. Sintering stages

The kinetics of the process can be broken down into three sintering stages:

2.8.1 Initial neck growth

Sintering initially causes the particles that are in contact to form grain boundaries at the point of contact through diffusion. This is the point contact stage and does not result in any dimensional changes. The greater the initial density of compaction (increased particle contact and potential grain boundary area), the higher the degree of coherency in the material. In this initial stage of sintering, necks begin to form at the contact points between adjacent particles figure 2-6. This stage is therefore referred to as the "neck growth" stage. No change in the dimensions is observed nor does porosity decrease [2,12].

Neck formation is driven by the energy gradient resulting from the different curvatures of the particles and the neck. Surface diffusion is usually the dominant mass-transport mechanism during the early stages of neck growth, as the compact is heated to the sintering temperature [14].

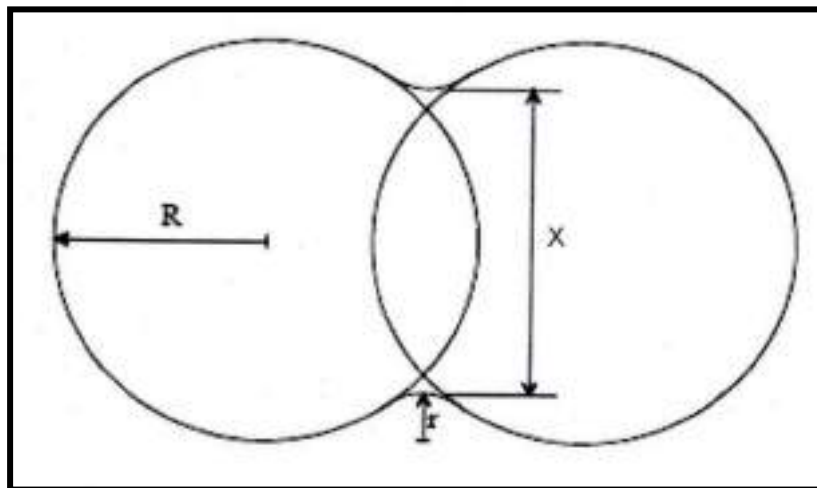


Figure 2-6 Neck formation [13].

2.8.2 Intermediate Stage Sintering

Intermediate stage sintering begins when adjacent necks begin to impinge upon each other. This occurs when the quantity $X/2R = 0.3$, figure 2-4. Densification and grain growth occur during this stage. The packing density and coordination number of the green packing are important during this stage. A high green packing density produces rapid sintering with relatively few pores in the final object [14].

The intermediate stage is pore channel closure where interconnected pore channels are closed off isolating porosity. One of the causes of pore channel closure is neck growth. Another cause is the creation of new contact points by pore shrinkage within the pore itself [2].

Coarsening processes was detailed in figure 2-5, very low green packing densities (around 40%), which are also associated with low coordination numbers which was shown in figure 2-7-a and 2-7-b. This was leading to coarsening (increase in mean grain size) without densification (decrease in porosity). In extreme cases, this may lead to open-pore structures lacking in structural integrity [14], as shown in figure 2-6-c.

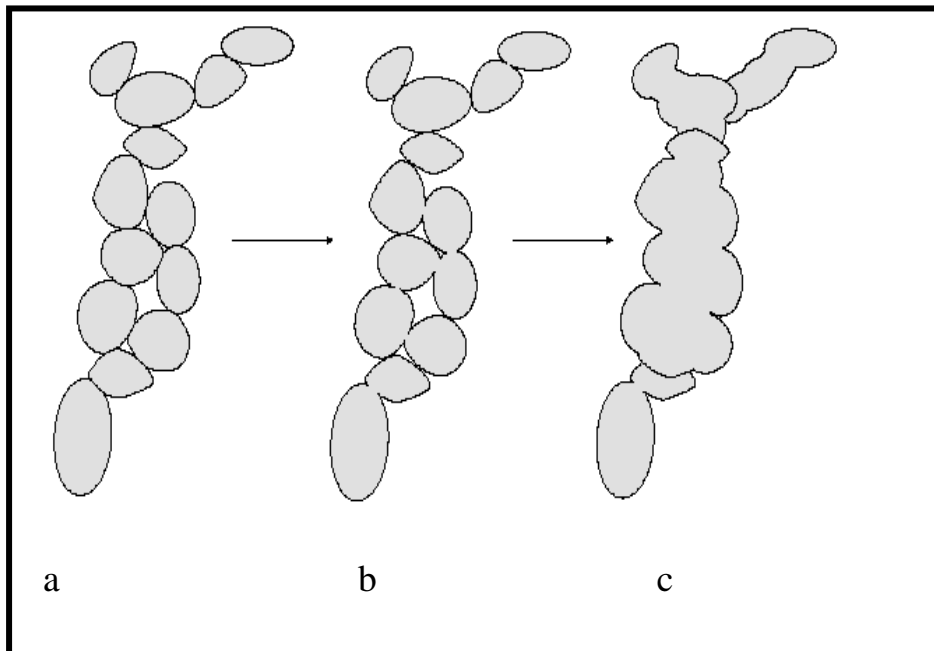


Figure 2-7 Coarsening resulting from low coordination number [14].

At the beginning of the intermediate stage, the pores form a network of interconnected cylindrical pores broken up by necks. By the end, the pores are smoother and begin to pinch off and become isolated from each other. Bulk transport mechanisms, such as grain boundary diffusion and volume diffusion, dominate the sintering process during this stage. As stated previously, these bulk transport mechanisms cause material to migrate from inside the particles to the surface, resulting in contact flattening and densification [14].

2.8.3 Final Stage Sintering

Final stage sintering begins when most of the pores are closed. As sintering proceeds, the pores, which during intermediate stage sintering form a network, have become isolated from each other [14]. Final stage sintering is much slower than the initial and intermediate stages. As grain size increases, the pores tend to break away from the grain boundaries and become spherical [14]. Pore shrinkage is the most important stage in sintering. For this stage to occur; solids must be transported into the pores and a means must exist by which the gas in the pores can escape to the surface. The resultant effect is to decrease the volume of the sintering mass. Grain boundary diffusion or lattice diffusion is usually the dominate mechanism during this stage [2].

Smaller pores are eliminated, while larger pores can grow, a phenomenon called ostwald ripening. In some cases, pore growth during final stage sintering can lead to a decrease in density, as gas pressure in the larger pores tends to inhibit further densification. This can be mitigated by having the final stage sintering occur into a partial vacuum [2].

2.9. Densification rate curves

Densification rate curves as a function of relative density are sensitive to microstructure, such as initial parameters of microstructure (agglomeration, pore size, heterogeneities) and heating schedule (thermal pre-treatment, heating rate). Densification rate curves can be correlated

with microstructural evolution during overall sintering and are expected to be a good help to choose raw materials [14].

The development of the densification rate curve model, specifically its predictive ability, is an important step toward the realization of the concept of "materials by design", i.e. to create the desired materials through designs based on our understanding of materials [14].

Figure 2-8 illustrates the densification in three stages of sintering. The density-time curve in the Figure is composed of three distinct portions. The first portion reflects the initial stage where densification is due to only neck growth. The densification in the intermediate stage is due to concurrent grain growth and reduced number of interconnected pores. When the pores are completely in the closed form, the rate of densification is reduced as shown in the final stage [14].

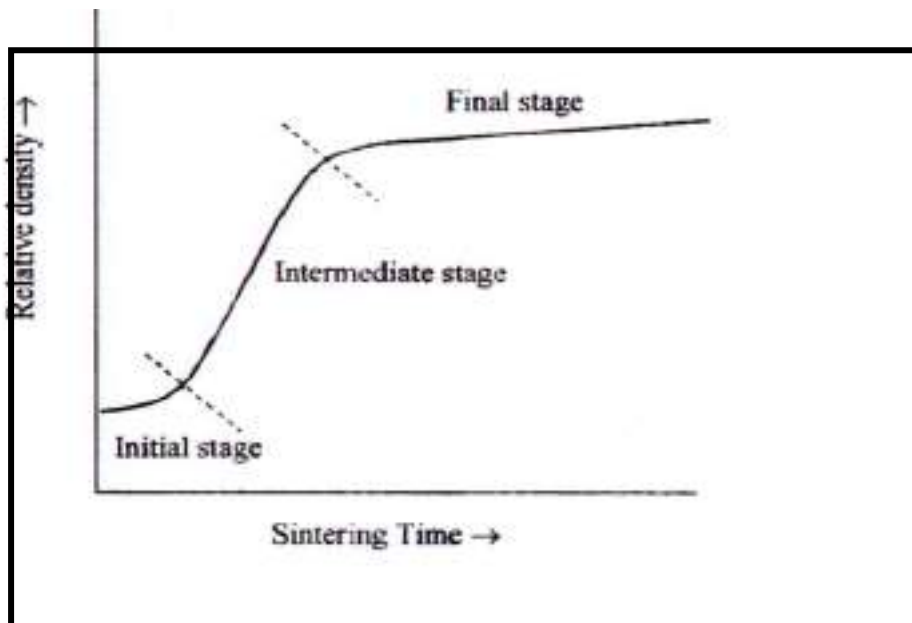


Figure 2-8 Typical densification curve [14].

Chapter three

Experimental part

Experimental Part

3.1. Introduction

The preparation techniques, supplies, and tools employed in this research are the main topics of this chapter. Powder technology using pressing and sintering that is one of the most significant manufacturing routes for ceramic or hard metal parts. It is not feasible to obtain a homogeneous green density distribution by die compaction, with the exception of the simplest part geometries. Depending on the component geometry, tool design, and friction between the powder and die wall, the density is more or less irregular. The mass of powder is fed slowly through a special high-temperature furnace to bind the particles together after it has been formed and expelled from the press. They undergo metallurgic-ally fusion also known as "sintering.

3.2. Used Materials

The raw materials used in this study, as the main component is Al₂O₃. TiO₂ and MgO, with the ratio that occurs in table (1)

Table (3-1) the Ratio of the component

Samples No.	Al ₂ O ₃	TiO ₂	MgO
A	100%	0	0
B	80%	20%	0
C	60%	20%	20%

3.3. Preparing Samples

3.3.1. Preparing Powder

The testing methods to produce the mixtures needed to achieve the goals stated in this Study samples made by combining the granules. Shown in figure (3-1) The powder must be test by using the following measurement such as: XRD and Particle Size..

AL₂O₃

MgO

TiO₂**Figure (3-1) Powder of AL₂O₃, MgO, TiO₂****Figure (3-2) Electrical Mixer**

3.3.2. Mixing Process

The powders of materials were mixed according to the mixing percentages by use the electrical mixer contains of strong plastic vessel and knives rotate with different speed Shown in figure (3-2) for (3) hour to obtain a homogeneous mixture.

3.3.3. Compacting

The mixture of powder was pressed into the form of a cylinder. performs several more important functions. The compression of the material decreases the proportion of voids in the mixture of powder. Pressing serves not only to give the samples its final size and shape. the applied load that used in the pressing the samples was 1 Mpa .Shown in figure (3-3) Liquid paraffin wax was used as the lubrication to reduce the friction between the two parts of the die and to prevent adhesion between the particles with die wall during getting out the sample from the die after the pressing. Polyvinal alcohol (PVA) binder was used to prepare the samples as the pressing is semi-dry.



Figure (3-3) Pressuring method

3.3.4. Drying

The next step after pressing was The samples were dried at temperature (110°C) for 24 hours by use the drying furnace which shown in figure (3-4) to remove the moisture from the samples which is available at the Babylon University/ College of Materials Engineering - Department of Ceramics and Building Materials.



Figure (3-4) Drying oven

3.3.5. Sintering

Sintering is generally considered successful when the process reduces porosity and enhances properties such as strength, electrical conductivity, translucency and thermal conductivity. In some special cases, sintering is carefully applied to enhance the strength of a material while preserving porosity (e.g. in filters or catalysts, where gas absorbency is a priority). During the firing process, atomic diffusion drives powder surface elimination in different stages, starting at the formation of necks between powders to final elimination of small pores at the end of the process. Shown the figure (3-5).



Figure (3-5) samples after sintering

3.4. Tests:

3.4.1. X- ray Diffraction test

X-Ray diffraction was used to characterize magnesia, alumina and Titania powders by (XRD) type (Shimadzo, XRD6000, diffractometer, Japon: X-Ray are generated using copper (Cu-K) radiation at 30KV, 40 mA and wave length $\lambda = 1.5406 \text{ \AA}$), radiation generating pattern of diffractions from powder sample at room temperature in 20 ranges of 20 to 80.

It is a rapid analytical technique, primarily used for phase identification of crystalline materials and also can provide information on unit cell dimensions. It is generated in cathode ray tube by heating a filament to produce accelerated electrons toward the target by applying high voltage. The interaction of the incident rays with sample produces constructive interference and diffracted ray when conditions satisfy the Bragg law

$$n\lambda = 2d \sin \theta$$

Where θ , is the angle of incidence of the x-ray. λ , is the wave length of the X-rays used and d is the spacing between atom layer. Figure (3-7 A) shows the apparatus of x-ray diffraction (XRD) type (Shimadzu 6000, Japan) which is available at the Babylon University / College of Materials Engineering – Department of Ceramics and Building Materials was used to characterize the structure of glass

The measurement conditions of the x-ray diffraction were:

Measure Conditions

X-ray

Target : Cu

Wave: 1.54060 (Å)

Voltage: 40.0 (KV)

Current: 30.0 (mA)

Slit

Divergence: 1.0 (deg)

Scatter: 1.0 (deg)

Receiving: 0.3 (mm)

Measure

Axis: Theta- 2 theta

Scan Mode: Continuous Scan

Range: 20.0 – 59.0 (deg)

Step: 0.02 (deg)

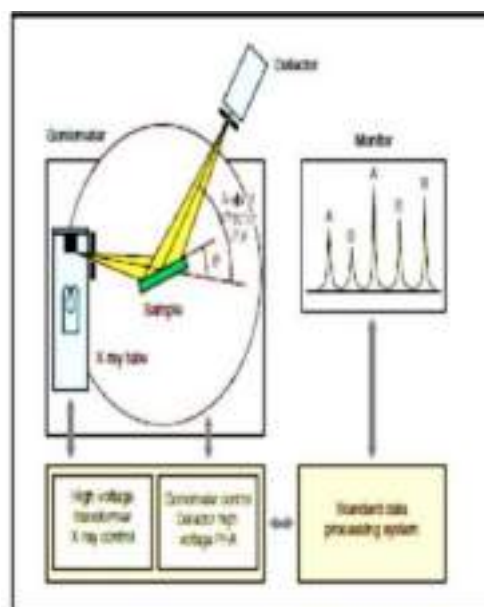
Speed: 7.0 (deg/min)

Preset Time: 0.17 (sec)

Subsequently, the powder of samples was prepared for XRD test after milling and sieving (mesh 200).



(A)



(B)

(3-6) A-Shimadzu 6000 X-Ray Diffraction (XRD), B-Working(Figure Principle

3.4.2. Particle size

Battersize 2000 laser particle size analyzer as shown in Figure (3-8) was used to measure particle size of samples at the Babylon University / College of Materials Engineering – Department of Ceramic and Building Materials. The measuring range can be selected between (0.02 μm -2000 μm). The principal operation of this device as shown in Figure (3-8) where during irradiation of the sample, a laser beam generates a diffraction pattern in which the laser light is deflected at various scatter angles depending on the grain size of the samples. Particles having the same size scatter at the same angle and the intensity of the scattered light provide information about the relative number of quantities of these particles. The angle and related intensity distribution are recorded by using a special multielement detector. A connected computer calculates the particles distribution in 31 channels according to grain size and percentage volume from diffraction patterns, which are generated during the measurement. According to these measurements, average particle size is determined. Fig (3-8) Battersize 2000 laser particle size analyzer.



Figure (3-7) Battersize 2000 laser particle size analyzer

3.4.3. Physical Test

3.4.3.1 Density

Bulk density (B), in grams per cubic centimeter of a specimen is the quotient of its dry weight divided by the exterior volume; including pores :

$$B=D/V \quad \dots\dots (3-1)$$

Where B is Bulk density, D is dry weight of the samples and V is the exterior volume of the samples.

3.4.3.2 Porosity

Apparent porosity is the percentage ratio of the volume of the open pores to the bulk volume of the specimen. Whereas, Water absorption is the percentage ratio of the weight have absorbed water in the pores to the weight of the solid part of the specimen. The apparent porosity and water absorption was measured as Archimedes method.

$$PA = [M-D]/ [M-S] *100 \quad \dots\dots (3-2)$$

Where:

PA = Apparent porosity.

M = Saturated weight to the specimen (g) after 24h in water.

D = Dry weight of the specimen (g).

S = Suspended weight of the specimen (g).

$$Wa= [M - D]/D *100 \quad \dots\dots (3-3)$$

Where:

Wa = water absorption (%)

3.4.3.3 linear shrinkage

Linear shrinkage on firing (L.S.%) was evaluated for samples by measuring the outer diameters of the samples before and after sintering

process (which are D1 and D2 respectively). Linear shrinkage (L.S.%) was calculated by the equation below according to (ASTM C326):

$$\text{L.S.}\% = \frac{D1-D2}{D1} \times 100\% \quad \dots\dots(3.4)$$

3.4.3.4 Absorption

This test was done by drying samples in drying oven at 110 °C for 24 hours, and then leaving them to cool at room temperature, and recording the dry weight for each sample by using a sensitive balance. Thereafter, samples were placed in glass flask, flooded with distilled water, then leave them immersed in water for 24 hours. then the sample's surface was dried from water drops that suspended on them by a piece of cotton cloth. Subsequently, the water saturated weight was recorded by using a sensitive balance.

Water absorption is the percentage ratio of the weight have absorbed water in the pores to the weight of the solid part of the specimen and could be fined by following equation (ASTM C1693-11)[64]:

$$A(\%) = \frac{M-D}{D} * 100 \quad \dots\dots (3-5)$$

Where:

A = absorption (%)

3.4.4. Mechanical tests

3.4.4.1 Hardness test

The hardness of samples was tested by Vickers hardness. Vickers hardness values were measured on surfaces by Vickers indentation technique at (10) kg load applied for (10) seconds using the device shown in figure (3-8) The Reading Diameter Rate Was Taken for Each Sample. The Following Law Was Adopted To Calculate The Vickers Hardness.

$$HV = 1.8544 \times \frac{p}{D2 \text{ average}} \quad \dots\dots (3-6)$$

Where:

HV: Vickers Hardness.

P: Applied Force (KG / MM).

D: AVERAGE DIAMETER (UM)



Figure (3-8) Microhardness device

3.4.4.2. Wear

Wear debris are produced when the plastic deformation exceeds the plasticity limit of the material, which is very limited for ceramics. As the tribological stress increases and reaches a critical point, various kinds of cracks (such as partial cone cracks, lateral/shallow cracks, and radial cracks etc.) are initiated.

Wear is the removal of the material from the surface of a solid body as a result of mechanical action of the counter body.

Chapter Four

Result and Discussion

Chapter four

Result and Discussion

4.1. Introduction

One of the most important production routes for ceramic or hard metal parts is powder technology by using pressing and sintering. Today, complex parts can be produced by (P/T) which were inconceivable just a few decades ago. Except for the very simplest part geometries, it is not possible to achieve a homogeneous green density distribution by die compaction. The density is more or less inhomogeneous depending on the part geometry, the tool design and the friction between powder and die wall.

After the mass of powder is squeezed into a shape and ejected from the press, it is fed slowly through a special high-temperature furnace to bond the particles together. They are metallurgically fused without complete melting, a phenomenon called "sintering"

This chapter discusses the results obtained for powders selected in chapter three.

4.2. X-Ray Test

The X-R-D test worked for choose samples that contained mixing powder for improvement the properties, material that we obtained (Alumina, Titania, magnesia).

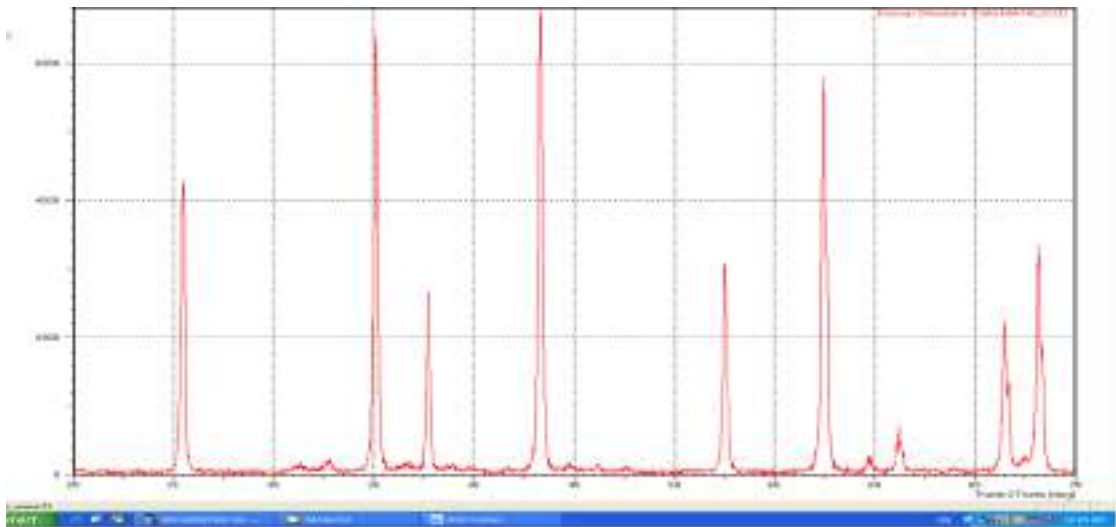


Figure (4-1): X-Ray for Al₂O₃

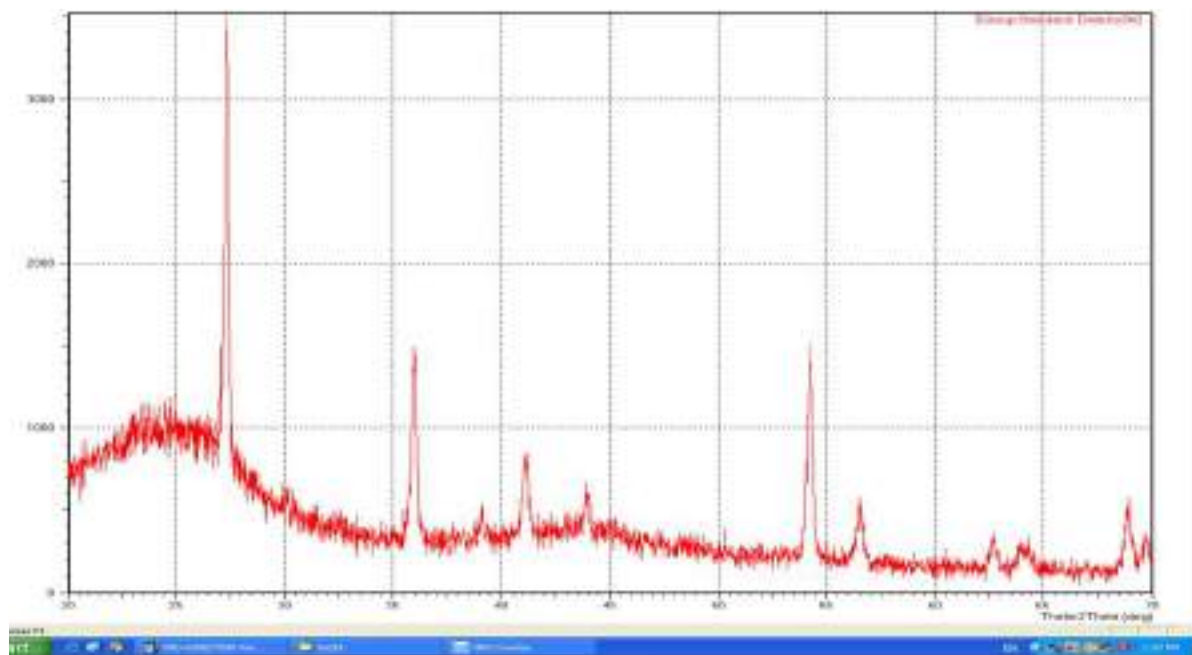


Figure (4-2): X-Ray for TiO₂

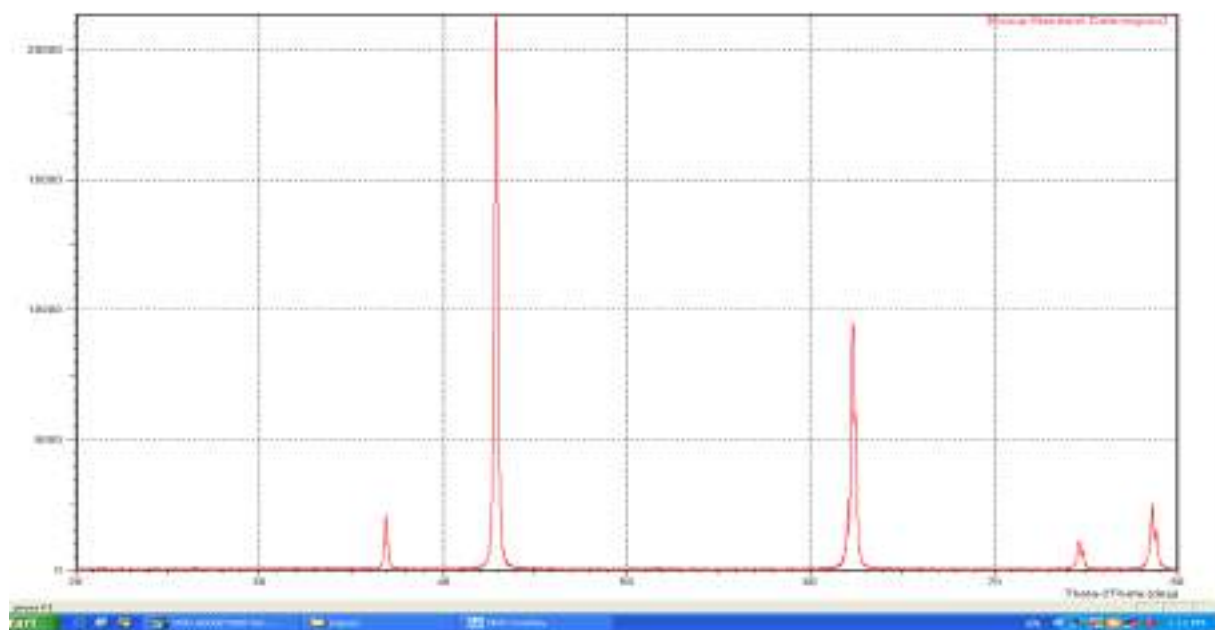


Figure (4-3): X-Ray for MgO

4.3. Particle Size for powders

The samples tested by using Bettersize2000 laser particle size analyzer, the results show that the particle size of Alumina is about 3.219 μm , titania is about 0.285 μm and for magnesia is about 3.437. Figure (4-4) shows the distribution of particles of Sample of Al_2O_3 , figure (4-5) shows the distribution of particles of Sample of Tio_2 and figure (4-6) shows the distribution of particles of Sample of MgO .

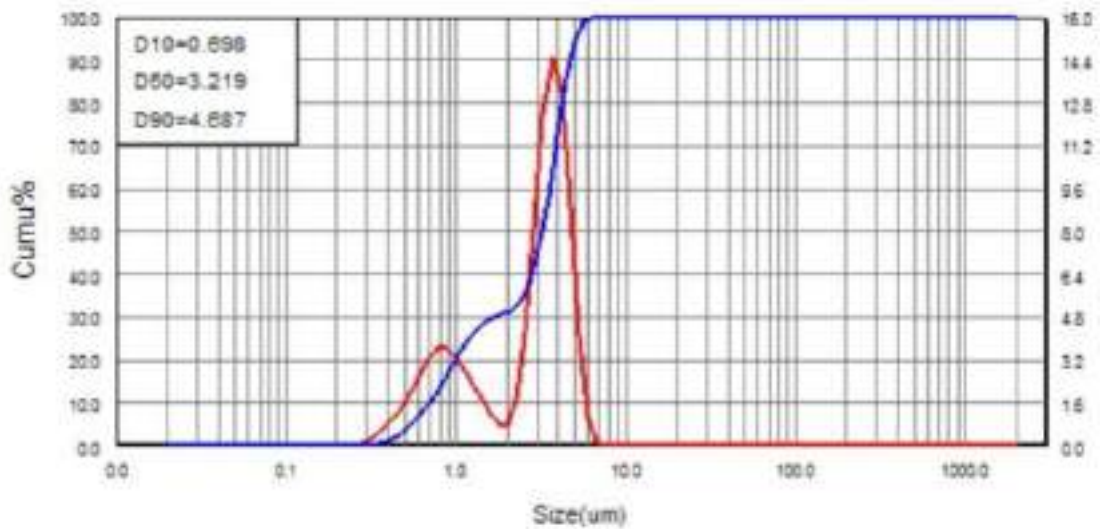


Figure (4-4) Particle size for Al_2O_3

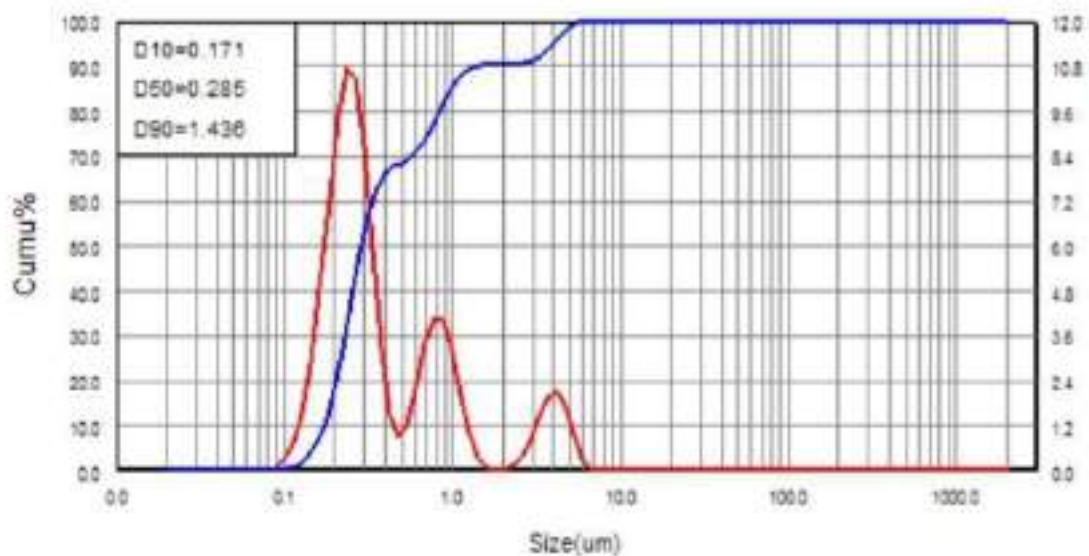


Figure (4-5) Particle size for Tio_2

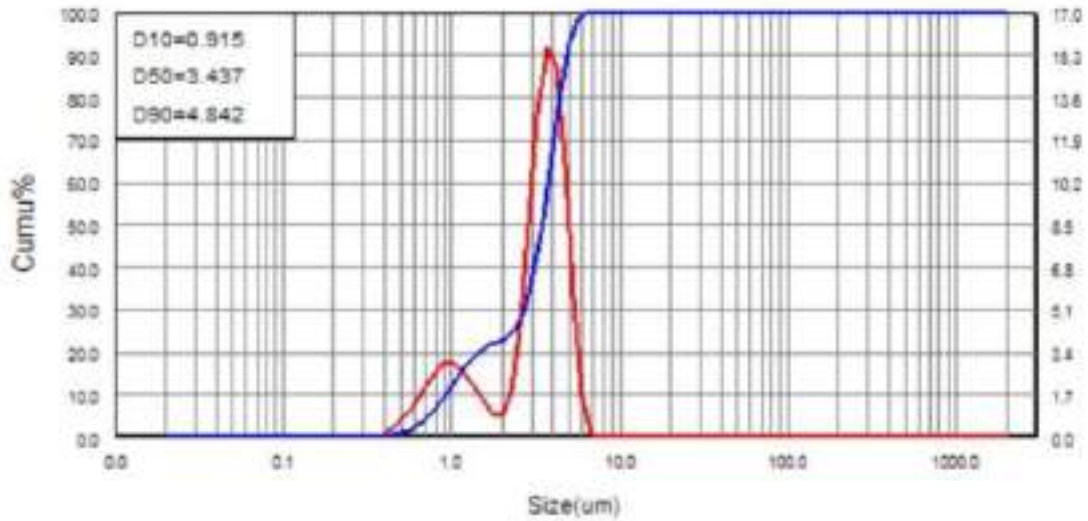


Figure (4-6) Particle size for MgO

4.4 Physical Testes

4.4.1 Density

The bulk density result of standard and mixing materials are shown in the table (4-1) and fig.(4- 7) , It can be noticed that density decreased by increasing the proportion of different addition. This behavior is expected due to the decline in porosity as mentioned below. the decrease in the density is the main reason behind the decrease in the mechanical properties such as hardness.

Table (4-1) Results of density

No. of sample	Al ₂ O ₃ %	TiO ₂ %	MgO%	Density g/cm ³
A	100	0	0	2.4
B	80	20	0	2.96
C	60	20	20	2.98

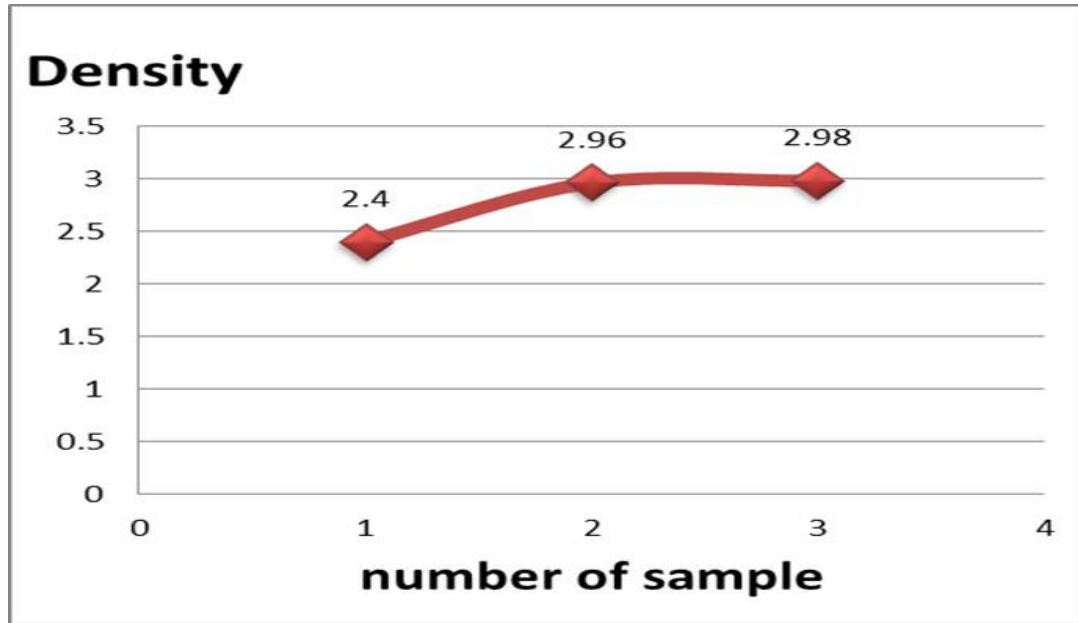


Figure (4-7) The relation between the samples and density

4.4.2 porosity

Table (4-2) shows the results of porosity for samples, and (Fig. 4-8) shows the relation between porosity with different addition of materials. The results show that the porosity decreased with decreasing ratio of alumina due to the different ratio of other materials which help in filling the pores of samples after sintering.

Table (4-2) results of porosity

No. of sample	Al ₂ O ₃ %	TiO ₂ %	MgO%	Porosity %
A	100	0	0	1.1
B	80	20	0	0.88
C	60	20	20	0.87

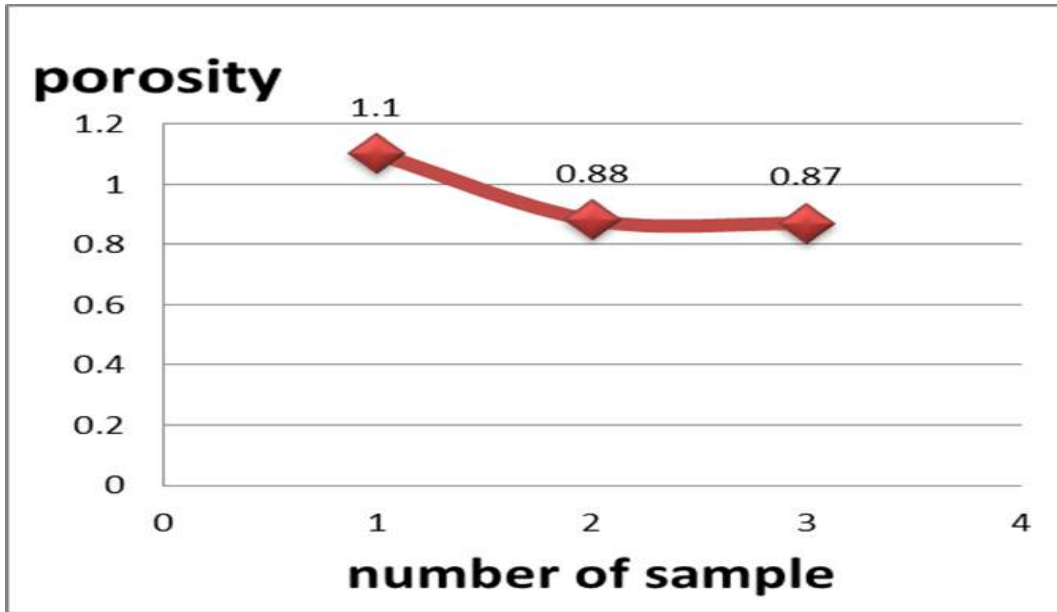


Figure (4-8) The relation between the samples and porosity.

4.4.3 Shrinkage

Table (4-3) shows the results of shrinkage for three samples, and (Fig. 4-9) shows the relation between shrinkage and samples with different addition of materials. The shrinkage increase as the porosity decrease with decreasing the absorption, whereas the density increase.

Table (4-3) Results of Shrinkage

No. of sample	Al ₂ O ₃ %	TiO ₂ %	MgO%	Shrinkage %
A	100	0	0	-2.96
B	80	20	0	-2.46
C	60	20	20	-1.91

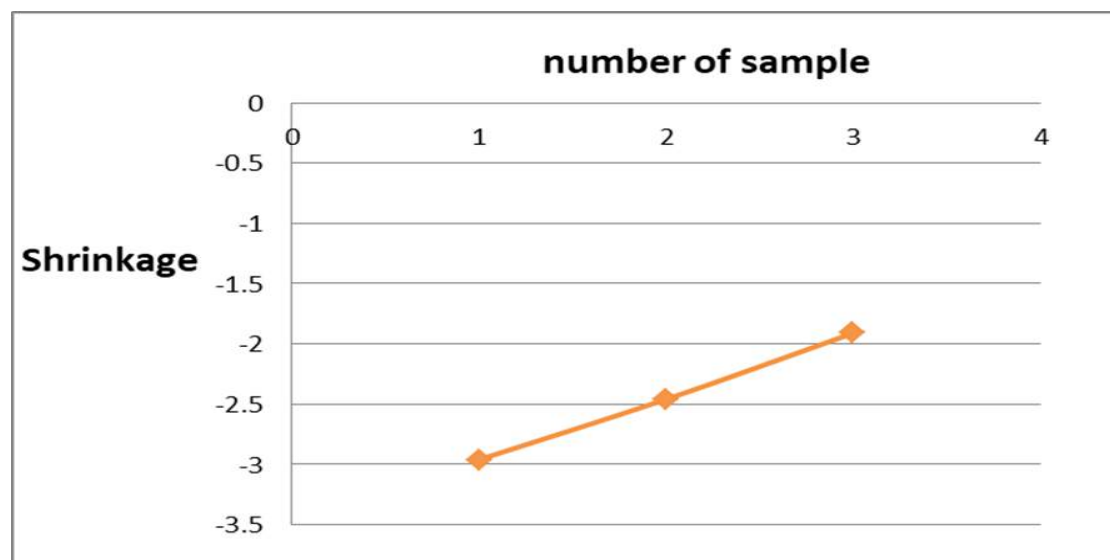


Figure (4-9) The relation between the samples and shrinkage.

4.4.4 Absorption

Table (4-4) shows the results of absorption for three samples, and (Fig. 4-10) shows the relation between porosity with different addition of materials. The results show that the absorption decrease with decreasing porosity, so the sample (c) show less absorption due to filling the porosity with the addition materials.

Table (4-4) results of Absorption

No. of sample	Al ₂ O ₃ %	TiO ₂ %	MgO%	Absorption %
A	100	0	0	45
B	80	20	0	43
C	60	20	20	42

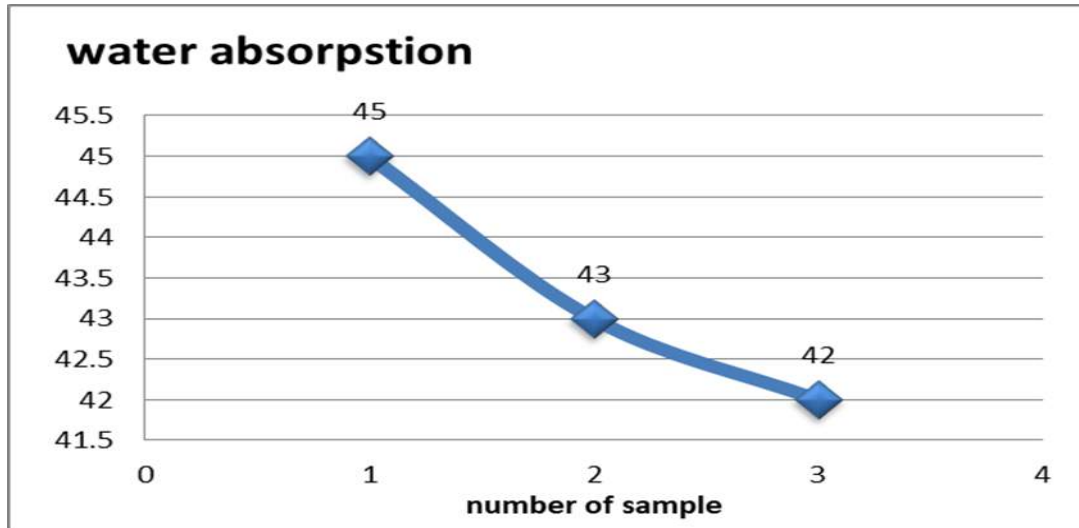


Figure (4-10) The relation between the samples and absorption.

4.5. Mechanical Testes

4.5.1. Hardness Test

The results of Vickers hardness test are shown in (Table 4-5), and (Fig. 4-11), so the figures below show the relation between tiania, magnesia addition and Vickers's hardness. It can be observed that the hardness increased by small degree significantly with the augmentation of the addition material percentage. Good bonding between the particles will appear with decreasing the porosity.

Table (4-5) Results in Vickers's hardness

No. of sample	AL ₂ O ₃ %	TiO ₂ %	MgO%	Hardness kg/mm ²
A	100	0	0	15.7
B	80	20	0	16.78
C	60	20	20	19.81

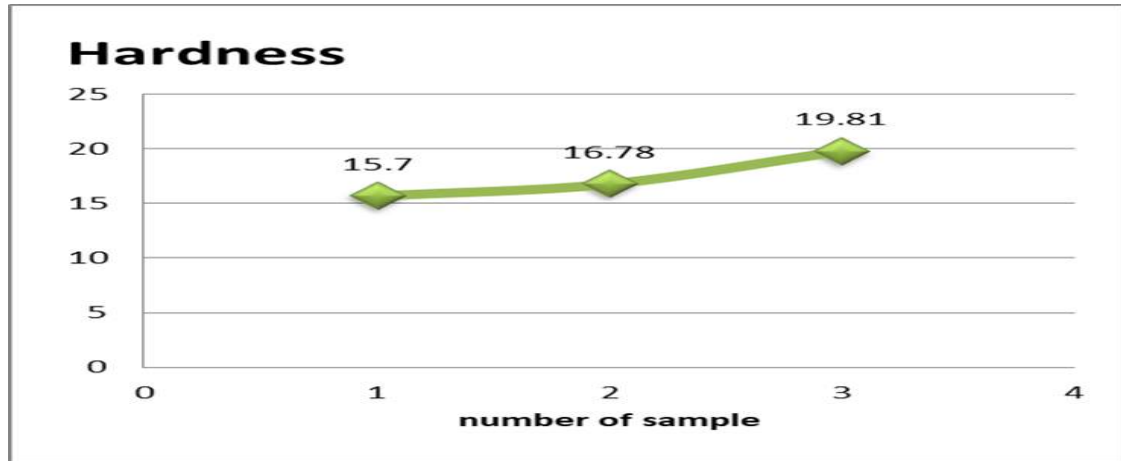


Figure (4-11) The relation between the samples and hardness

4.5.2. Wear Test

The results of wear test are shown in (Table 4-6) (Table 4-7) (Table 4-8) and (Fig. 4-12) (Fig. 4-13) (Fig. 4-14) shows the relation between three samples and wear tests. The samples with low hardness have high value of wear that is clear in figures below.

Table (4-6) The relation between the samples (Al_2O_3) and Wear

Time	W(gram)	Δw
0	3.862	
5	3.8185	0.0435
10	3.7115	0.1505
15	3.6875	0.1745
20	3.5737	0.2883

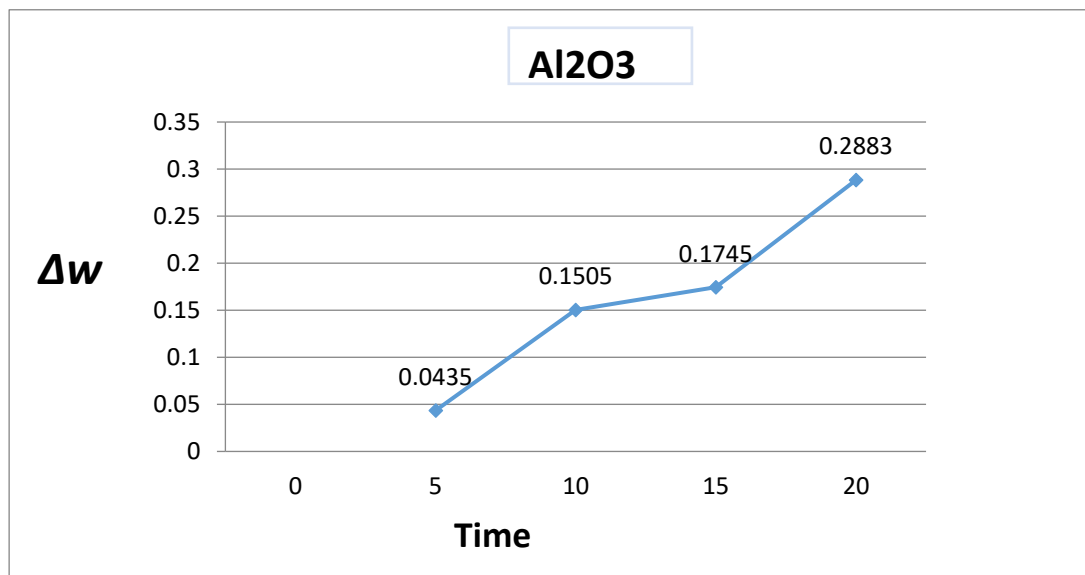
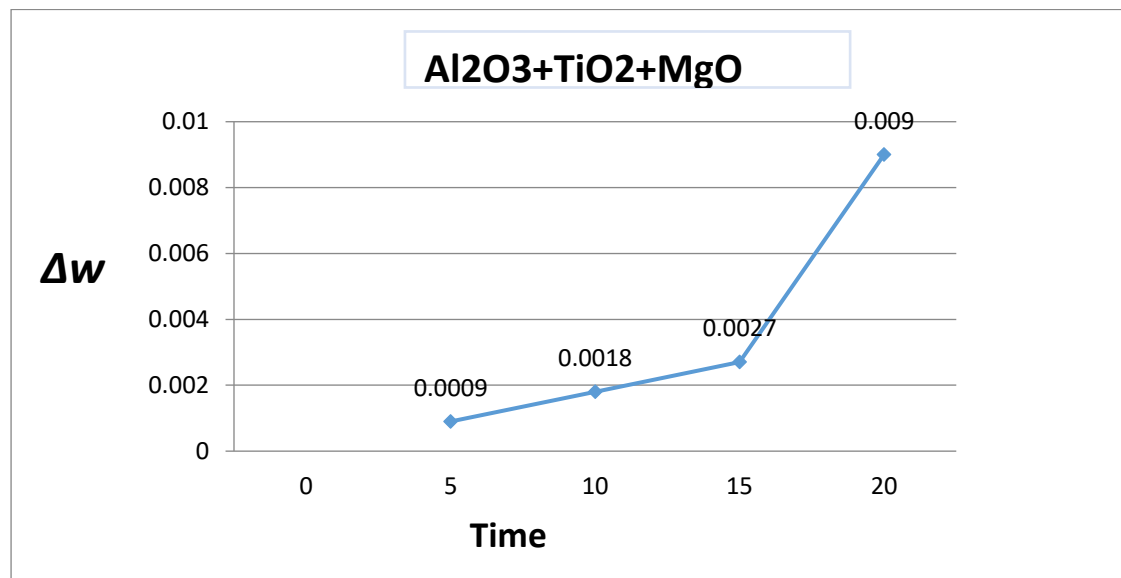


Figure (4-12) The relation between the samples (Al₂O₃) and WearTable(4-7) the relation between the samples (Al₂O₃+TiO₂+MgO) and Wear

Time	W	Δw
0	5.333	
5	5.3324	0.0009
10	5.3315	0.0018
15	5.3306	0.0027
20	5.3243	0.009

Figure (4-13) The relation between the samples (Al₂O₃+TiO₂+MgO) and WearTable (4-8) the relation between the samples (Al₂O₃+TiO₂) and Wear

Time	W	Δw
0	4.6208	
5	4.6198	0.001
10	4.6144	0.0064
15	4.6138	0.007
20	4.126	0.0082

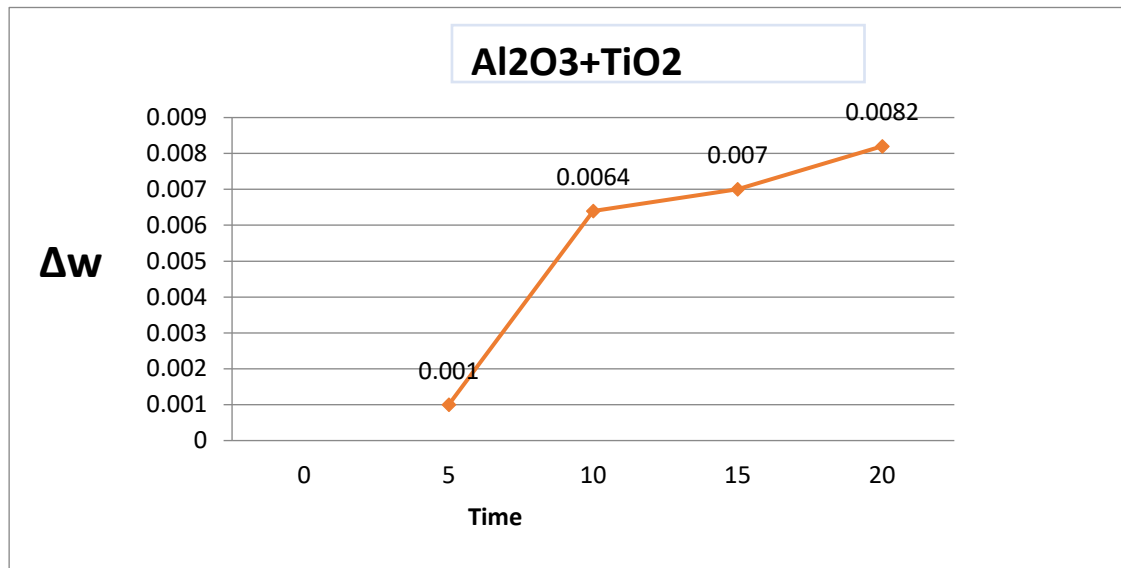


Figure (4-14) The relation between the samples ($\text{Al}_2\text{O}_3+\text{TiO}_2$) and Wear

Chapter Five

Conclusions and Recommendations

Chapter five

Conclusion and Recommendation

5.1. Conclusion

The following conclusions obtained are from the sintering process for mixing material.

1-Improvement in density is achieved for sample (A), (B) and (C) are about (2.4 g/cm^3), (2.96 g/cm^3) and (2.98 g/cm^3) respectively.

2- The value of porosity for composite materials samples (B) and (C) (1.1%), (0.88%), (0.87%) respectively are lower than pure material sample (A).

3- Shrinkage values, for pure material sample (A) is about (-2.96%) and for the sample (B) and (C) are about (-2.46%) and (-1.91%).

4- Absorption for samples (A), (B) and (C) seems to be as (45%), (43%) and (42%) respectively, which related to porosity of material

5-Hardness values, of pure material, sample (A) and for samples (B) and (C) about (15.7 Hv), (16.78 Hv) and (19.81Hv) which related directly to the density of materials.

6. wear play good roll in this study, the value of three samples decrease as hardness increase.

5.2. Recommendations and suggestions for future work

Because of the importance of the composite material and for further work in this field for achieving better results, the following suggestions are presented.

1 -Studying the effect of mixing by other different ratios of titania and magnesia with alumina on the physical and mechanical properties.

2- By using vacuum sintering, studying the effect of a different proportion of these material on the physical and mechanical properties.

3- Studying the effect of mixing these materials on the other properties, especially the thermal properties.

References

References

- [1] C. Ferguson, Historical Introduction to the Development of Material Science and Engineering as a Teaching Discipline, (2001).
- [2] Dolores Eliche-Quesada, Luis Pérez-Villarejo and P. J. Sánchez-Soto, Introduction to Ceramic Materials: Synthesis, Characterization, Applications, and Recycling, 2019.
- [3] M. M. Schwartz, Encyclopedia of Materials, Parts and Finishes, 2nd edition, CRC Press LLC, New York, (2002).
- [4] J. Ernesto Indacochea, Mat E 272, Lectures 22-23: Introduction to Ceramic Materials, November 26 & 28, (2001).
- [5] A.C. Harper, Handbook of ceramics, Glasses and Diamonds, McGraw-hill Inc, U.S.A., (2001).
- [6] C. C. Barry and Norton M. Grant, Ceramic Materials science and engineering, Springer, P. 7, (2007).
- [7] R. Riedel, E. Ionescu and I.-Wei Chen, Modern Trends in Advanced Ceramics, Ceramics Science and Technology. Vol.1: Structures., (2008).
- [8] M. N. Rahaman, Ceramic Processing and Sintering, 2nd edition, Marcel Dekker, Inc., New York, (2003).
- [9] M. F. Ashby and D. R. Jones, Engineering Materials an Introduction to Microstructures, Processing and Design, 2nd edition, Butterworth - Heinemann publishing, (1998).
- [10] K. Hashimoto, H. Irie, and A. Fujishima, "TiO₂ photocatalysis: A historical overview and future prospects," Japanese J. Appl. Physics, Part 1 Regul. Pap. Short Notes Rev. Pap., Vol. 44, No. 12, PP. 8269–8285, 2005.

- [11] A. J. Haider, Z. N. Jameel, and I. H. M. Al-Hussaini, "Review on: Titanium dioxide applications," *Energy Procedia*, Vol. 157, PP. 17–29, 2019, doi: 10.1016/j.egypro.2018.11.159
- [12] A. K. Rana, S. B. Rana, A. Kumari, and V. Kiran, "Significance of Nanotechnology in Construction Engineering," *Int. J. Recent Trends Eng.*, Vol. 1, No. 4, PP. 6–8, 2009.
- [13] Shamsudin, S. Ahmad, M. K. Aziz, A. N. Fakhriah, R. Mohamad, F. "Hydrophobic rutile phase TiO₂ nanostructure and its properties for self-cleaning application," *AIP Conf. Proc.*, Vol. 1883, No. September, 2017, doi: 10.1063/1.5002048.
- [14] S. Wahyuningsih, R. E. Cahyono, F. N. Aini, and A. H. Ramelan, "Preparation Titanium Dioxide Combined Hydrophobic Polymer with Photocatalytic Self-Cleaning Properties," *Bull. Chem. React. Eng. Catal.*, Vol. 15, No. 3, PP. 874–884, 2020, doi: 10.9767/BCREC.15.3.9225.874-884.
- [15] C. Buzea, I. I. Pacheco, K. Robbie, and C. Buzea, "Nanomaterials and nanoparticles : Sources and toxicity Nanomaterials and nanoparticles : Sources and toxicity," Vol. 17, No.2007, 2016, doi: 10.1116/1.2815690.
- [16] R. Riedel and I. Chen, *Ceramics science and technology: Materials and Properties*, Vol. 2, 2008.
- [17] M. Mohamad, B. Ul, R. Ahmed, A. Shaari, N. Ali, and R. Hussain, "Materials Science in Semiconductor Processing A density functional study of structural , electronic and optical properties of titanium dioxide : Characterization of rutile , anatase and brookite polymorphs," *Mater. Sci. Semicond. Process.*, Vol. 31, pp. 405–414, 2015, doi: 10.1016/j.mssp.2014.12.027.
- [18] Rupesh Kumar, Vishnu Prabhakar, and Jasmeen Saini, *Alumina*, international Journal of Current Engineering and Technology, Vol.3, No.5,(2013).

[19] Lidija Ćurković , Ivana Ropuš , Hrvoje Cajner ,Sanda Rončević and Ivana Gabelica , StatisticAl₂O₃ ptimisation of Chemical Stability of Hybrid Microwave-Sintered Alumina Ceramics in Nitric Acid, *Materials*, 15(24), 8823, 2022.

[20] P. Maheswaran, Alumina properties,(2021).

[21] Erdem Uzun and Yasemin Yarar, Characterization of Alumina Ceramics, Conference: First Hellenic-Turkish International Physics Conference, 2001.

[22] Yajun Zheng, Xiaoling Zhang, Zongquan Bai and Zhiping Zhang, Characterization of the surface properties of MgO using paper spray mass spectrometry, *LibraryRapid Commun. Mass Spectrom*, 30(Suppl. 1), 217–225, 2016.

[23] Jonathan Amodeo, Sébastien Merkel, Christophe Tromas, Philippe Carrez, Sandra Korte-Kerzel, Patrick Cordier, Jérôme Chevalier, Dislocations and Plastic Deformation in MgO Crystals: A Review, *Crystals*, 8 (6), PP.1-53, 2018.

[24] Magnesia - Magnesium Oxide (MgO) Properties & Applications, AZO materials.

[25] P. Samal, J. Newkirk, Powder Metallurgy, ASM International, ISBN electronic: 978-1-62708-175-7, 2015.[26] Dr. M. Sayuti, powder metallurgymetallurgy , ST., M.Sc, the blessing university.

[27] Ritwik Sarkar and Goutam Bannerjee, Effect of addition of TiO on reaction sintered MgO–Al₂O₃ spinels, *JournAl₂O₃ f the European Ceramic Society*, Vol. 20, Issue 12, Pages 2133-2141,(2000).

[28] Liang Li, Effect of Mineralizers on Sintering Properties of MgO-Al₂O₃-SiO₂ Composite Ceramics, *Proceedings of the Nineteenth China International Nanoscience and Technology Symposium*, Vol. 215, Issue 1,(2021).

-
-
- [29] Oksana M. Borysenko , Galina M. Shabanova , Sergey M. Logvinkov , Lgor A. Ostapenko , Thermodynamic Modeling Of MgO-Al₂O₃- TiO₂ System, China's Refractories, Vol.30, Issue 3, PP.17-22, (2021).



جمهورية العراق
وزارة التعليم العالي والبحث العلمي
جامعة بابل
كلية هندسة المواد
قسم السيراميك و مواد البناء

دراسة خصائص الألومينا بعد
إضافة نسب مختلفة من التيتانيا والمغنيسيا

رسالة

مقدمة إلى كلية هندسة المواد/جامعة بابل كجزء من متطلبات نيل
درجة البكالوريوس في هندسة المواد/ قسم السيراميك ومواد البناء

من قبل

محمد علي شهيد

بإشراف

أ.د. ألهم عبد المجيد

د. اسيل هادي

